J Radioanal Nucl Chem (2013) 298:33–39
DOI 10.1007/s10967-012-2225-9

Finding a suitable shield for mixed neutron and photon fields based on an Am–Be source

Keyhandokht Karimi-Shahri · Laleh Rafat-Motavalli · Hashem Miri-Hakimabad

Received: 28 June 2012 / Published online: 26 September 2012

Abstract This study aimed to investigate a shielding design against neutron and photon rays from neutron irradiators based on Am–Be sources, using the Monte Carlo simulation. Different shielding materials were studied, including borated polyethylene, DaGa concrete, and epoxy resin with colemanite. The Monte Carlo N-particle code (MCNP) was used to design shielding. A new type of neutron and photon shielding material based on 40 % galena, 55 % polyethylene, and 5 % boric acid is proposed. The results show that the total effective dose of radiation is significantly reduced by the optimum radius of this shielding system.

Keywords Shielding design · Am–Be source · Neutron effective dose · ORNL phantoms · Monte Carlo simulation

Introduction

With the increasing use of radiation for variety of application, the human body is exposed to different levels of radiation energy. Therefore, the risks associated with radiation exposure increased in human body. For this reason, a major current challenge in radiation protection is finding techniques to reduce the dose of exposure; designing high performance shielding materials is crucial in achieving this goal. This is particularly important for radiation sources that emit neutron and photon radiations because these rays are very penetrating. Moreover, the effect of neutrons must be considered due to their highly destructive effects on the body (especially in low energies). The radioactive isotope Am–Be is the most important neutron source and has been used efficiently for many applications in medicine [1, 2], industry [3, 4] and scientific research [5, 6]. Designing an appropriate shielding mechanism is essential in preventing exposure of Am–Be radiation because of its very long half life ($t_{\frac{1}{2}} = 432.7y$) [7] and its supply of high neutron and photon flux multiple shielding mechanism are needed for Am–Be sources because captured neutrons and photons have a wide range of energies [8, 9] that must be considered. Monte Carlo codes have effective roles in solving this problem. Neutron energies from Am–Be source can be classified into four groups: thermal ($E < 500$ eV), epithermal (500 eV $< E <$ 10 keV), fast (10 keV $< E <$ 1 MeV) and ultrafast ($E >$ 1 MeV) neutrons, photon energy groups have similar energies: $E <$ 500 eV, 500 eV $< E <$ 5 MeV and 5 MeV $< E <$ 15 MeV.

It is first necessary to decrease the speed of neutrons from fast to thermal energy by employing appropriate shielding materials. The process of decrease the speed of neutrons is mostly achieved by elastic collisions with light nuclei such as hydrogen. The thermal neutrons are then absorbed by the shielding material. Shielding materials most commonly used include polyethylene, paraffin, water barite concrete [10, 11], and colemanite [12]. Recently heavy concrete consist CoGa concrete [13] and DaGa concrete [14], which are mainly composed of large amounts of hydrogen, has also been used. Hydrogen is a suitable moderator for neutrons at energies below 10 MeV, making it a good candidate as a shielding material for Am–Be sources. Materials such as boric acid and boron carbide, which have high boron content, have also been utilized to absorb neutron energy.

In addition to neutrons, Am–Be provides a large photon flux. Photons from Am–Be source can be classified in two

K. Karimi-Shahri · L. Rafat-Motavalli · H. Miri-Hakimabad (✉)
Physics Department, School of Sciences, Ferdowsi University of Mashhad, 91775-1436 Mashhad, Iran
e-mail: mirihakim@ferdowsi.um.ac.ir

categories: photon rays that are directly created by the source and photon rays produced by a neutron-gamma (n,γ) reaction when shielding materials capture thermal neutrons. This latter group of photons is a secondary source of radiation and must be shielded. The photon shielding is chosen according to linear attenuation coefficients and the mass density. Most photon rays are in the compton region; therefore, shielding materials should have high inelastic scattering properties to send more photon rays to lower energy regions. Lead, tungsten, bismuth, and recently natural rock under the name of galena are candidates as the material for photon shielding.

Materials and methods

Calculation procedure

The purpose of the present study was to investigate an optimum shielding arrangement of materials using a simulation study on the ORNL adult mathematical phantom [15–17]. In fact, the ORNL phantom is a modified MIRD model, which has been used for various calculations [18–20]. The phantom was placed at a distance of 150 cm from the Am–Be source and irradiated under an AP field. Energy spectrum data were taken from an IAEA report 403 [21] for neutron rays and from the Miri et al. [22] report for gamma rays.

The Monte Carlo radiation transport code Monte Carlo N-particle code (MCNP) was used for all calculations. Calculations were performed on personal computers with the following specifications: Intel(R) Core(TM) i7 CPU 3.07 GHz processor, 6.00 GB of RAM and Windows7 (64 bit). The evaluated nuclear data came from the ENDF/B-VI cross-section library; including the appropriate thermal neutron scattering function $S\ (\alpha, \beta)$ and photon library. Energy cut off values of 10^{-9} and 0.01 MeV were considered for neutrons and photons, respectively. A PWT card was used in the simulated programs. By using this card, secondary photons were transported only in the phantom and ignored in other cells. Results of these programs were utilized for calculations of the equivalent dose. Because neutron and secondary photon organ doses can be produced from neutron interactions with body tissues, they should be summed and then multiplied by neutron radiation weighting factors (w_R) for calculation of the neutron equivalent dose. The tallies that were used as a program output were: F1 tally which is a surface current tally that counts the number of particles for estimation of the mean radiation weighting factor, F4 tally, the volume flux, for calculation of the red bone marrow absorbed dose, and F6 tally for estimating the amount of deposited energy in different organs and tissues. The thickness of the shielding device was 70 cm. These shields were generated as concentric spheres with different radii. A general view of this set up is shown in Fig. 1.

New tissue and radiation weighting factors, w_T and w_R, from the ICRP 103 recommendation were used to calculate the whole body effective dose [23]. The following formula was applied for average effective dose estimations

$$E = \sum_{T} w_T \left[\frac{H_{T,\,male} + H_{T,\,female}}{2} \right] \quad (1)$$

All calculations were performed for people in the public sector, such as a laboratory operator or person, who work around the laboratory, considering 73 working hours in a month. Although concrete walls are usually utilized in laboratories, 1.5 m from the source was considered a close distance to the public. But these conditions were considered to provide a safe distance of protection.

Neutron and gamma shielding

Polyethylene and polyethylene mixed boric acid is widely used as an effective neutron shielding material. Some of the materials used for neutron and gamma shielding in simulations are shown in Tables 1 and 2. The last layer of the shield must be the photon shield because these are gamma secondary sources that must be shielded.

Several designed shields are summarized in Table 3.

Shields that contain polyethylene and concrete, such as 30 cm polyethylene(PE),70 cm mixed polyethylene with 5 % boric acid PE-B), and 70 cm ordinary concrete(OC), are usually used to shield Am–Be source moreover, 70 cm heavy concrete (DaGa), which was constructed from Datolite and Galena minerals, was studied. This concrete had a

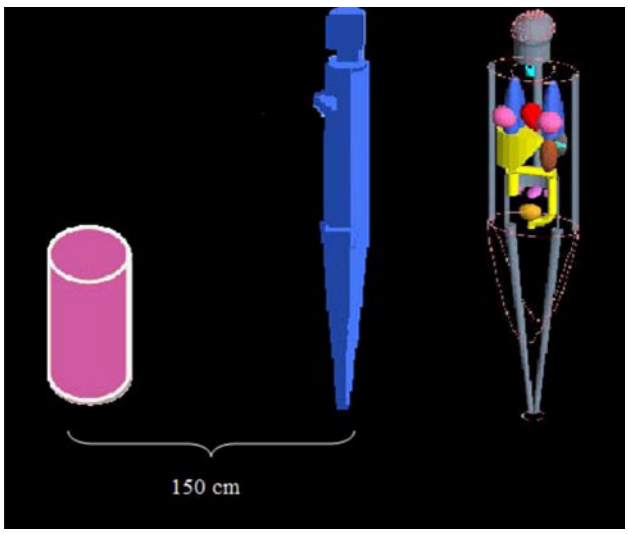

Fig. 1 A general view was drawn from the simulated geometry. It should be noted here that the plotted shape of the ORNL female phantom is Geant 4 out put

Table 1 Typical neutron shielding materials

Material	Density (gr cm^{-3})	Chemical formula	References
Ordinary concrete	2.5	[a]	[29]
Datolite-galena (DaGa) concrete	4.420–4.650	[b]	[14]
Colemanite-galena (CoGa) concrete	4.100–4.650	[c]	[13]
Ulexite	1.95	$NaCaB_5O_6(OH)_6{\cdot}5(H_2O)$	[30]
Colemanit	2.42	$CaB_3O_4(OH)_3{-}H_2O$	[13]
Datolite	2.9	$CaBSiO_4(OH)$	[14]

[a] Oxygen 52.9 %, silicium 33.70 %, calcium 4.4 %, aluminum 3.4 %, sodium 1.6 %, iron 1.4 %, potassium 1.3 %, hydrogen 1 %, magnesium 0.2 %, carbon 0.1 %

[b] Galena 64.16 %, datolite 16.20 %, cement 17.18 %, microsiliceus 1.72 %, distilled water 0.0074 %

[c] Galena 63.93 %, colemanite 16.14 %, cement 17.12 %, microsiliceus 1.7 %, distilled water 1.09 %

Table 2 Typical gamma shielding materials

Material	Density (gr cm^{-3})	Chemical Formula
Tungsten	7.4	W
Bismuth	9.78	Bi
Galena	7.2	PbS
Lead	11.34	Pb
Iron	7.87	Fe
Nickel	8.91	Ni

density of 4.420–4.650 gr/cm^3, which is much higher than that of ordinary concrete (2.3–2.5 gr/cm^3). One of the important properties of galena concrete is a high compressive strength (approximately 4.48–5.22 gr/cm^3) [14].

Recently, a new type of neutron shielding material based on epoxy resin and colemanite was proposed. Therefore, a next shield material composed of mixing 50 cm epoxy resin and colemanite [24] with two layers of 10 cm galena placed on both sides, was designed and its shielding performance was estimated (GERCG). The main characteristics of epoxy resin are good dimensional stability and chemical proof. Colemanite is a neutral rock that contains boron oxide [12]. Studies on neutron shielding materials using colemanite have been reported for more than 40 years. Galena is also the main mineral in lead [14].

The new shield was designed by using two layers of 10 cm bismuth located on two sides of ordinary concrete with 50 cm thickness (BiOCBi). Similar to this shield, another shield was designed in which bismuth layers were placed within the galena layers (GOCG). Other shields were made with a layer of tungsten with 20 cm thickness that was placed before (WPE-B) and after (PE-BW) 50 cm mixed polyethylene with 5 % boric acid, respectively.

Table 3 Different configurations of selected shields, their prices in Iran versus world price

Configuration	Thickness	Average effective dose (mSv y^{-1})	Price in Iran $	World price $
Phantom bare	–	46.560	–	–
PE	30 cm	1.994	260	180
OC	70 cm	0.552	460	500
DaGa	70 cm	0.411	8,000	60,000
GERCG	10 cm/ 50 cm/ 10 cm	0.549	7900	7900
BiOCBi	10 cm/ 50 cm/ 10 cm	0.424	300,000	100,000
GOCG	10 cm/ 50 cm/ 10 cm	0.449	2,800	4,100
WPE-B	20 cm/ 50 cm	0.0564	31,000	11,000
PE-BW	50 cm/ 20 cm	0.005	700,000	200,000
WBCPE-B (frequently)	5 cm/ 18 cm/ 5 mm	0.002	300,000	90,000
PE-B	70 cm	0.220	3,000	2,000
GPE-B	70 cm	0.068	3,700	3,100

Shielding designs using multiple layers and homogeneous mixtures of several materials were also analyzed, such as a shield composed of multi layers of tungsten, polyethylene and boron carbide. This shield contains four layers of 5 cm tungsten, eight layers of 5 mm boron carbide, and 46 cm mixed polyethylene with 5 % boric acid that include two layers of 18 cm and a layer with 10 cm thickness (W-BCPE-B). The last shield is a homogeneous mixture of 55 % polyethylene, 40 % galena, and 5 % boric acid (GPE-B).

Results

All calculations in this work have a statistical uncertainty of less than 3 %. To achieve this uncertainty, 2×10^9 particle was transported.

The effects of these shields were investigated from two views. Firstly, the contributions of incident neutrons and photons were specified in total effective doses (Fig. 2). As previously noted, the neutron effective dose also contains secondary photon doses. Secondly, it was necessary to

determine the origin of photons emission. Figure 3 shows the effective dose values for photons that were emitted by an Am–Be source; photons enter the body directly and are produced from neutron interactions with body tissues.

The average effective dose for all shields is summarized in Table 3, for the rate of source emission considered at 10^7 n s^{-1}. The third column in this table shows the price of suggested shields in Iran and their world price based on reputable sites is given in the fourth column [25–27]. Obviously, the price of the shield will be changed in each country with considering that whether it is importer or exporter for the specific material of the shield. For example, Iran is one of the biggest exporters of galena. Therefore, galena has a cost-effective use in Iran.

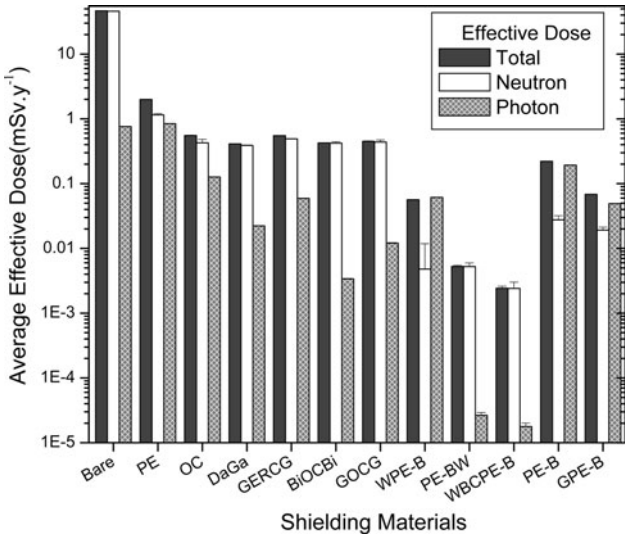

Fig. 2 Total, neutron, and photon effective doses are shown for the different set-ups. The neutron effective dose contains the effective dose evaluations of neutrons and secondary photons produced in body tissues. The photon effective dose represents photon doses that enter the body directly

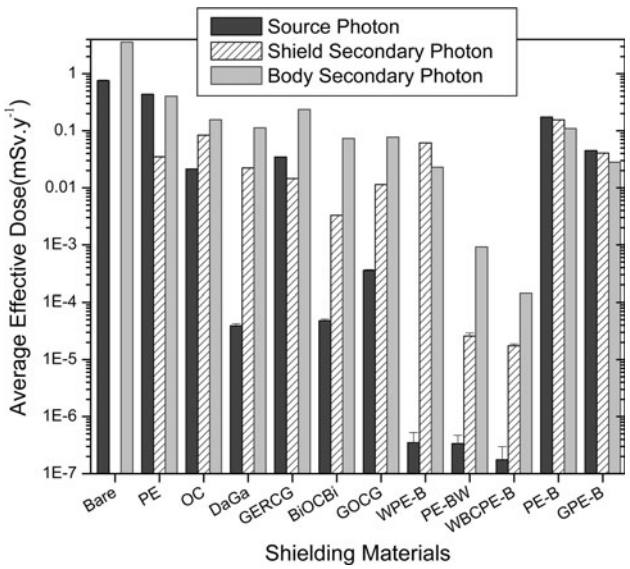

Fig. 3 Effective dose evaluations are shown for source photons, and, secondary photons in the shield and in body tissue. Shield and body secondary photons are photons that are produced from neutron interactions with shields and the body, respectively

Table 3 illustrates that an effective dose value of less than 0.6 mSv y^{-1} for all set-ups in AP irradiation conditions except, in the bare phantom, and in the standard shield i.e. 30 cm polyethylene,.

The lowest dose obtained with the multi-layer shield of WBCPE-B at which the effective dose value was approximately 2.4 μSv annually.

In addition to the decrease in the dose evaluation, a good shield should be inexpensive and readily available as possible. Tungsten and boron carbide, compared to other materials, are both expensive; therefore the use of these materials to make a shield, due to financial consideration, is not suitable.

Various compositions were designed from the different percentages of galena, polyethylene, and boric acid. These shielding systems contained 20–60 % of galena. After comparing the results, the effective dose values decreased with increasing galena percentage, with a 7 % dose reduction for a galena increase from 20 to 40 %. However the effective dose remains constant when the amount of galena rises from 40 to 50 % but increases by 8 % with a galena composition of more than 50 %. It is noted that the impurity of silver is 600–2000 ppm for the available galena in Iran. Considering this impurity does not significantly change the results (the discrepancy between these results with acquired data from pure galena is less than 2 %). For this reason, galena can be considered without impurity.

Different percentages of boric acid were investigated in similar shields. The analysis shows that the total effective dose of polyethylene mixed with 5 % boric acid is less than that of the same shield with 10 % boric acid.

This study proposed a shield compose of a homogenous compound of 55% polyethylene, 40 % galena, and 5 % boric acid (Table 3). The effective dose evaluation decreases to 0.068 mSv y^{-1} by applying this shield.

Discussion

The analysis of the current results for every set-up will be discussed to understand the factors associated with efficiency of shielding design.

Tungsten is used in both WPE-B and PE-BW shield, with 20 cm thickness. However, the tungsten is placed before the polyethylene in WPE-B and immediately after polyethylene in the PE-BW. In accordance with the results presented in Table 3, the effective dose value obtained in

PE-BW is less than that obtained using the WPE-B by approximately 11 times. As shown in Fig. 2, the main reason of this discrepancy is found in the photon effective dose data. Figure 3 illustrates that emerged photons from the shield are a large contribution of the photon effective dose in WPE-B. Indeed, placement of the photon shield (w) before the neutron shield cannot shield photons produced by neutron interactions with the polyethylene, this photon shield can only cover photons that are emitted directly by the source. Photons that are produced in polyethylene can be shielded by changing the tungsten position (PE-BW). However, secondary photons created in body tissues cannot be shielded in this set-up. In addition, a major problem occurs by shifting tungsten from the front to the end of the set-up: the gamma-shielding materials are displaced and have a high density. Therefore, if the gamma-shielding materials are moved to the end of the set-up, a large volume is occupied by them, creating a major problem. For example, a shield with 20 cm tungsten (WPE-B) generates a volume of 33.510 m^3 versus 913.16 m^3 in PE-BW. With this method, the designed set-up becomes heavy, and more expensive, making the choice of tungsten unattractive. Although, as expected, the best shielding results were yielded when tungsten was used in the shied (Table 3).

The results of this study provide an idea on the position of gamma shields that can affect set-up weight and shield photons. To distribute a gamma-shield between neutron shields, it can be placed on two sides of the polyethylene (a layer with 10 cm thickness before and a second layer after) or a homogenous mixture can be applied(GPE-B).

Tungsten was replaced by other materials such as iron, nickel, lead and bismuth in primary calculations. However, these materials generated large secondary photons, i.e., they acted as a gamma source when exposed to a neutron source, thus worsening the radiation exposure. For this reason, galena was preferred. However, the galena density is less than that of lead, but has a higher cross-section for neutron absorption due to sulfur (Fig. 4). The sulfur existence in galena not only absorbs more neutrons than lead, but also reduces the production of neutron induced photons in the shield. Indeed, galena is a consolidated shield for neutron and gamma rays.

Although bismuth is better than galena as gamma shield, as results show, the effective doses of secondary photons produced in body tissues by BiOCBi set-up are 0.73 versus 0.77 mSv y^{-1} in GOCG. In addition, the effective doses of photons created in shields are 0.003 and 0.01 mSv y^{-1} for bismuth and galena set-ups, respectively. The photon effective doses of BiOCBi is also less than GOCG (4.78×10^{-5} vs 3.56×10^{-4} mSv y^{-1}). The difference in the total effective dose between BiOCBi and GOCG in comparison with the large difference in photon dose is

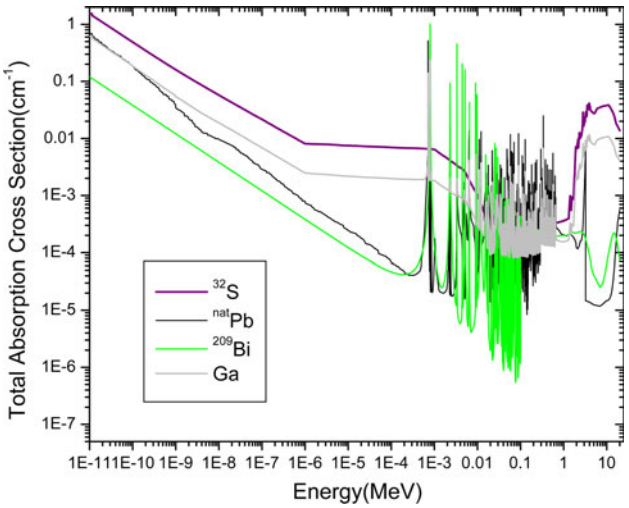

Fig. 4 Comparison of total neutron absorption cross- section for bismuth, lead, and galena plotted against neutron energy. The galena absorption cross section is clearly higher than that of bismuth and lead

small (approximately 12 %). Because the neutron effective dose, which is a main contributor to the total effective dose, has the same value in both set-ups. Despite this dose difference (12 %), galena was chosen as a convenient photon shield due to the fact that bismuth is heavier, harder, and significantly more expensive than galena.

Indeed, these results revealed the influence of neutron shielding on the appropriate selection of the gamma shield. Thus the design of a high performance shield is complex.

The source photon contribution is small in all designed shields but is non-negligible in shields of PE, PE-B and GPE-B. In these shields, the main contribution to the photon effective dose is devoted to the source photon. Considering that radiation weighting factors are 1 for these photons, they hold a small fraction of the total effective dose.

In this study, the proposed shield is a homogenous mixture of GPE-B with 70 cm thickness. The total effective dose obtained from this shield is lower than that of DaGa concrete by approximately 6 times. In addition, the proposed shield performs better than common shields such as OC and PE-B by almost 8 and 3 times, respectively.

Increasing galena to 40 % in GPE-B decreased the total dose, but increasing the galena percentage further increased the total effective dose. This may be explained by the following. The composition of polyethylene in a shield with 40 % galena is 55 %. The results show that 55 % polyethylene is the saturation threshold for this composition. Indeed, polyethylene plays the role of the moderator and absorber in these compositions, converting fast neutrons to thermal ones, thereby decreasing the neutron flux. When the polyethylene composition is more than 55 % (65, 75,…), the contribution of galena is reduced, therefore photons are not shielded and

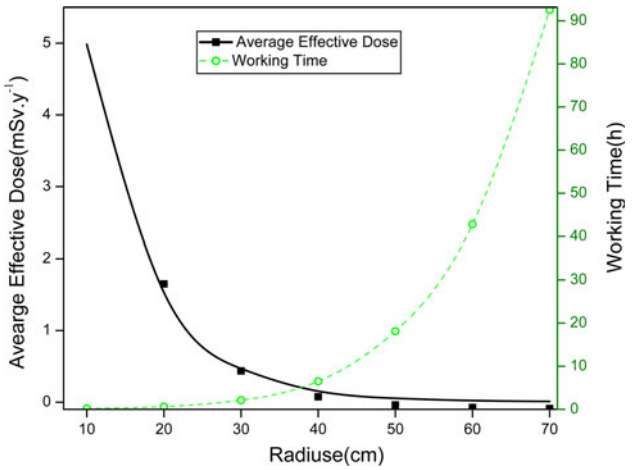

Fig. 5 The evaluation of effective doses and the working time are compared for cylinders with different radiuses and heights. The shield material is the same for all cylinders: 40 % galena, 55 % polyethylene and 5 % boric acid

can reach the body. In addition, some fast neutrons cannot be thermal, when the percentage of polyethylene reaches 45 % (50 % galena). Thus, some neutrons leave the shield without interacting with the materials, and enter the body. For this reason, the effective dose increases.

Nevertheless, the use of every listed shield with the exception of 30 cm polyethylene reduces the effective dose evaluation below the annual accepted dose for the public. However, in laboratories at which several sources are used coincidently, further reduction in the effective dose is necessary.

In order to find the optimum radii for the proposed shield, different cylinders were designed with the same height and diameter. Figure 5 shows the estimation of the average effective dose per one source particle and in the permitted daily working hours considering 1 mSv y^{-1} as the acceptable annual dose for the public [28] for shields with radiuses of 10, 20, 30, 40, 50, 60, and 70 cm. A radius of 40 cm was selected as the optimum radius at which the effective dose value is approximately 0.51 mSv y^{-1} and the public can work a 6.5 h day with a 1.5 m distance from the source. The shield radius was decreased to about 15 cm with respect to an 8-h working day and 20 mSv y^{-1} of the acceptable annual dose for occupational workers [28]. To make this shield with a 40 cm radius 30, 240, and 330 kg of boric acid, galena, and polyethylene are needed, respectively. The world price of this shield is almost 800 $ while it costs about 1000 $ in Iran.

Conclusion

Although Am–Be is a neutron source, only applying a neutron shield cannot supply protection. Therefore, gamma shielding is essential tor this aim. Moreover, the position of the gamma shield is important because it is determines the set-up weight and which gamma types are covered. A suitable solution is to distribute gamma shields between neutron shields. In addition, the total price of materials needed, should be appropriate for financial considerations.

According to the results, the GPE-B had the overall best shielding abilities among the materials investigated for the mixed neutron and gamma fields based on an Am–Be source. The optimized radius of this shield is estimated at approximately 40 cm, with an the average effective dose of 0.51 mSv y^{-1} for this set-up.

Acknowledgments This study was supported by a grant from the Ferdowsi University of Mashhad (p/449-26/7/1388).

References

1. Elis KJ (1993) In vivo activation analysis: present and future prospects. J Radioanal Nucl Chem 169:291–300
2. Morgan WD (2000) Of mermaids and mountains. Three decades of prompt activation in vivo. Ann N Y Acad Sci 904:128–133
3. Zimbal A (2007) Measurement of the spectral fluence rate of reference neutron sources with a liquid scintillation detector. Radiat Prot Dosim 126:413–417
4. Rezaei-Ochbelagh D, Miri-hakimabad H, Izadi-Najafabadi R (2007) The investigation of Am–Be neutron source shield effect used on landmine detection. Nucl Instrum Methods A 577:756–761
5. Khelifi R, Amokrane A, Bode P (2007) Detection limits of pollutants in water for PGNAA using Am–Be source. Nucl Instrum Methods B 262:329–332
6. Khelifi R, Bode P, Amokrane A (2007) Flux calculation in LSNAA using an ^{241}Am–Be source. J Radioanal Nucl Chem 274:639–642
7. Mowlavi AA, Koohi-Fayegh R (2004) Determination of 4.438 MeV γ-ray to neutron emission ratio from a ^{241}Am–^{9}Be neutron source. Appl Radiat Isot 60:959–962
8. Magalotti N, Lacoste V, Lebreton L, Gressier V (2007) Investigation of the neutron energy distribution of the irsn ^{241}Am–Be(α, n) source. Radiat Prot Dosim 125:69–72
9. Vega-Carrillo HR et al (2002) Neutron and gamma-ray spectra of ^{239}PuBe and ^{241}AmBe. Appl Radiat Isot 57:167–170
10. Bouzarjomehri F, Bayat T, Dashti RM et al (2006) ^{60}Co gama-ray attenuation coefficient of barite concrete. Iran J Radiat Res 4:71–75
11. Akkurt I, Basyigit C, Kilincaslan S (2006) Radiation shielding of concrete different aggregates. Cem Concr Compos 28:153–157
12. Yarar Y, Bayulken A (1994) Investigation of neutron shielding efficiency and radioactivity of concrete shielding containing colemanite. J Nucl Mater 212-215(B):1720–1723
13. Mortazavi SMJ, Mosleh-Shirazi MA, Roshan-Shomal P et al (2010) High-performance heavy concrete as a multi-purpose shield. Radiat Prot Dosim 142(2–4):120–124
14. Mortazavi SMJ, Mosleh-Shirazi MA, Baradaran-ghahfarokhi M et al (2010) Production of a Datolit-based heavy concrete for shielding nuclear reactors and megavoltage radiotherapy rooms. Iran J Radiat Res 8:11–15
15. Snyder W, Ford M., Warner G, Fisher HJ (1987) Estimates of absorbed fractions for monoenergetic photon source uniformly distributed in various organs of a heterogeneous phantom medical

internal radiation dose committee (MIRD) pamphlet no. 5 revised. The Society of Nuclear Medicine, New York
16. Cristy M, Eckerman K (1987) Specific absorbed fractions of energy at various ages from internal photon sources Report No. ORNL/TM-8381Nl. Oak Ridge National Laboratory, Oak Ridge
17. Ulanovsky AV, Eckerman KF (1998) Absorbed fractions for electron and photon emissions in the developing thyroid fetus to five years old. Radiat Protect Dosim 79:419–424
18. Manger RP, Bellamy MB, Eckerman KF (2011) Dose conversation coefficients for neutron exposure to the lens of the human eye. Radiat Protect Dosim 29:1–7
19. Lee C, Lee C, Eun YH (2007) Consideration of the ICRP 2006 revised tissue weighting factors on age-dependent values of the effective dose for external photons. Phys Med Biol 52:41–58
20. Lee C, Lee JK (2006) Computational anthropomorphic phantoms for radiation protection dosimetry: volution and prospects. Evol Nucl Eng Technol 38:239–250
21. International Atomic Energy Agency (2001) Compendium of neutron spectra and detector responses for radiation protection purposes. Technical reports series No. 403. IAEA Publication
22. Miri-Hakimabad H, Panjeh H, Vejdani-Noghreiyan A(2007) Shielding studies on a total-body neutron activation facility Iran. J Radiat Res 5:45–51
23. ICRP Publication103 (2007) The 2007 recommendations of ICRP. Elsevier, Amsterdam, pp 1–332
24. Kratt C, Coolbaugh M, Calvin W (2006) Remote detection of quaternary borate deposits with ASTER satellite imagery as a geothermal exploration tool. GRC Trans 30:435–439
25. Metal Price Pages (2012) http://www.metal-pages.com/metalprices/minors/
26. Chemical prices and chemical industry trends from ICIS pricing (2012) http://www.icispricing.com/il_shared/Samples/SubPage143.asp
27. (2012) http://www.alibaba.com/
28. ICRP Publication116 (2010) Conversion coefficients for radiological protection quantities for external radiation exposures. Elsevier, Amsterdam, pp 1–257
29. Analytical Chemistry Laboratory (ACL) of Ferdowsi University of Mashhad, Iran (2007)
30. Okuno K (2005) Neutron shielding material based on colemanite and epoxy resin. Radiat Protect Dosim 115:258–261